Three modeling methods in MFL testing

Zuoying HUANG, Peiwen QUE
Department of Instrument Science and Engineering
Shanghai Jiaotong University; Shanghai, P.R.China
Phone: +86 21 34205295, Fax: +86 21 34204392;
e-mail: hzuoying@sjtu.edu.cn, pwque@sjtu.edu.cn

Abstract

Magnetic flux leakage (MFL) measurement is one of the most widely used non-destructive testing techniques for in-service inspection of oil and gas pipelines. Three methods, Numerical computation, theory analytical and experiment, have been used to model the MFL testing and have been investigated separately before. In this article, we introduced a MFL analytical model based on dipole magnetic charge method, a MFL Numerical model base on three dimensional FEM. Test equipment and samples were designed and produced to make a MFL experiment model, the results by three models were analysis. We summarized the advantages and disadvantages of three different methods and discussed.

Keywords: MFL, analytical model, numerical model, FEM

1. Introduction

The magnetic flux leakage (MFL) method is currently the most commonly used gas pipeline inspection technique. MFL method detects defects by applying a magnetic field in the pipe wall. When a ferromagnetic material is subjected to a magnetic field, irregularities in the pipe can cause the induced flux to leak out into the adjacent air. The magnetic leakage field measured on the nearby of the pipe contains information about the pipe conditions.

Three methods, Numerical computation, theory analytical and experiment, have been used to model the MFL testing and have been investigated separately before. The analytical model of MFL is based on the theory of Zatsepin and Shcherbinin. They approximated defects as point, line and strip magnetic dipoles, and the MFL signal induced by the magnetic polarization at the walls of a defect. Some researchers developed the model and considered variation of conditions[1-3]. 2D finite element methods have been used to research MFL signals under different defects shapes, materials, magnetizing situation and so on and it is also proved to be an effective method[4,5]. However, in 2D FEM defects are also treated as 2D profile instead of actually 3D geometry, and the result MFL signal is single channel whereas the actual signals are multi-channel. In this paper, 3D FEM is adopted to analyze the MFL method, accurate 3D defect are modeled and detail MFL signal in test surface are calculated by the method. We also introduce an experiment apparatus and the results.

2. Analytical model of MFL

A cylindrical defect shown in Figure.1 was considered. The central axis of the defect

was along with z-axis and the applied magnetic field direct was along with y-axis. The center of defect located at the origin point of xy plane. The defect was general filled with non-ferromagnetic material whose permeability is very close to that of air. The magnetic field lines diverge around the low permeability flaw, inducing a dipole magnetic charge on the walls of the cylindrical. Reverse magnetic polarities appeared on the walls of the cylinder divided by zx plane. The charge was assumed to be distributed homogeneously on the cylinder,

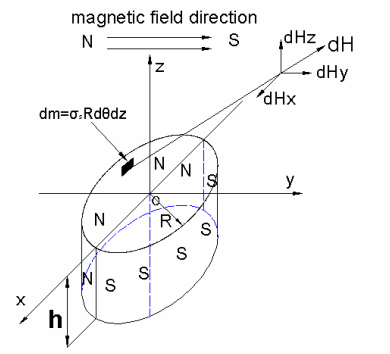

Figure 1. Defect dipole model

The cylindrical defect has a radius R and depth h. The angle θ is measured from the positive x axis to magnetic charge. The sensor has a lift-off value l. the magnetic charge density of cylinder is denoted by σs, half of the cylinder has positive magnetic charge while the other half has a negative magnetic charge because of different magnetic polarities. The differential element of charge, dm, is given by[6]

$$dm = \sigma_s R d\theta dz$$

The charge density σs is assigned a value of 1. The magnetic field generated at a distance r by the charge dm is given by [5]

$$\overset{\mathrm{r}}{dH} = \frac{dm}{4\pi r^3} \cdot \overset{\mathrm{r}}{r}$$

The MFL signal of inspection area, the position parallels to xy plane and has positive z coordinate value, are analyzed in this paper. Initially, the positive polarity part of the defect is considered. As shown in figure 1, the distance r_p from the charge dm to any inspection point is

$$r_p = \left[(x - R\cos\theta)^2 + (y + R\sin\theta)^2 + (l - z)^2 \right]$$

Combining equation □-□, the y and z components of the field at a distance r_p are given by

$$dH_z^p = \frac{Rd\theta dz}{4\pi r_p^3}(l - z)$$

$$dH_y^p = \frac{Rd\theta dz}{4\pi r_p^3}(y + R\sin\theta)$$

The z component of magnetic field by the positively polarized side of cylinder can be attained by integrates the area.

$$H_z^p = \frac{R}{4\pi}\int_0^{\pi}\int_{-b}^{0} \frac{(l-z)}{\left[(x-R\cos\theta)^2+(y+R\sin\theta)^2+(l-z)^2\right]^{3/2}} dzd\theta$$

By integrating the dz element, magnetic field H_z^p is given by

$$H_z^p = \int_0^{\pi}\left(\frac{1}{\sqrt{(x-r\cos\theta)^2+(y+R\sin\theta)^2+h^2}} - \frac{1}{\sqrt{(x-r\cos\theta)^2+(y+R\sin\theta)^2+(h+b)^2}}\right)d\theta$$

The same method is applied to the negatively polarized side of the cylinder except that the path of integration is in counter clockwise direction. Because of the changing of polarity and position, the magnetic leakage field can be given by changing equation to

$$H_z^n = -\frac{R}{4\pi}\int_0^{\pi}\int_{-b}^{0} \frac{(l-z)}{\left[(x-R\cos\theta)^2+(y-R\sin\theta)^2+(l-z)^2\right]^{3/2}} dzd\theta$$

Similar to equations and , the y component of magnetic leakage field are given by equations and .

$$H_y^p = \frac{R}{4\pi}\int_0^{\pi}\int_{-b}^{0} \frac{(y+R\sin\theta)}{\left[(x-R\cos\theta)^2+(y+R\sin\theta)^2+(l-z)^2\right]^{3/2}} dzd\theta$$

$$H_y^n = -\frac{R}{4\pi}\int_0^{\pi}\int_{-b}^{0} \frac{(y-R\sin\theta)}{\left[(x-R\cos\theta)^2+(y-R\sin\theta)^2+(l-z)^2\right]^{3/2}} dzd\theta$$

the total magnetic leakage field is given by

$$H_z = H_z^p + H_z^n$$

$$H_y = H_y^p + H_y^n$$

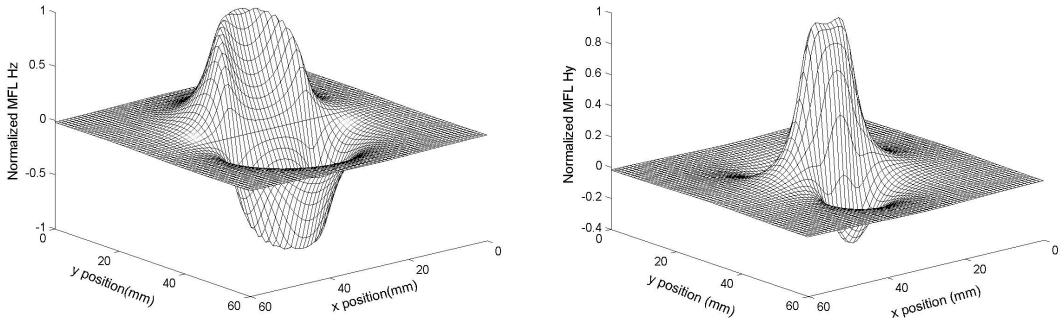

(a) z component (b) y component

Figure 2. Theoretical normalized MFL for type a defect

Figure 2 shows the MFL simulation result of a cylinder defect. The diameter of defect is 10mm and the depth is 8mm. There are a peak and a valley in the picture of z component MFL signal by cylinder defect and a peak in y component. The simulating results are

consistent to experiment.

3. Three-dimensional finite element computation of MFL numerical models

The MFL problem can be treated as magnetostatic problem by magnetic scalar potential method. It can be expressed by Maxwell's equations below[7]:

$$\nabla \times \{H\} = \{J_s\} \tag{1}$$

$$\nabla \cdot \{B\} = 0 \tag{2}$$

where {H} is magnetic field intensity vector, {Js} is applied source current density vector and {B} is magnetic flux density vector.

The field equations are supplemented by the constitutive relation that describes the behavior of electromagnetic materials.

$$\{B\} = [\mu]\{H\} + \mu_0\{M_0\} \qquad \text{in permanent magnet region} \tag{3}$$

$$\{B\} = [\mu]\{H\} \qquad \text{in other region} \tag{4}$$

where μ is magnetic permeability matrix, {Mo} is remnant intrinsic magnetization vector.

In the domain of a magnetostatic field problem, a solution is sought which satisfies the Maxwell equation (1),(2) and the constitutive relation (3) in the following form: [7, 8]

$$\{H\} = \{H_g\} - \nabla\phi_g \tag{5}$$

$$\nabla \cdot [\mu]\nabla\phi_g - \nabla \cdot [\mu]\{H_g\} - \nabla \cdot \mu_0\{M_0\} = \{0\} \tag{6}$$

where $\{H_g\}$ is preliminary magnetic field, ϕ_g is generalized potential.

The development of {Hg} varies depending on the problem and the formulation. Basically, {Hg} must satisfy Ampere's law so that the remaining part of the field can be derived as the gradient of the generalized scalar potential ϕ_g. This ensures that ϕ_g is singly valued. Additionally, the absolute value of {Hg} must be greater than that of $\Delta\phi_g$. In other words, {Hg} should be a good approximation of the total field. This avoids difficulties with cancellation errors.

The finite element matrix equations can be derived by variational principles. The element matrices of scalar potential can be presented in the following form:

$$\left[K^m\right] = \left[K^L\right] + \left[K^N\right] \tag{7}$$

$$\left[K^L\right] = \int_V \left(\nabla\{N\}^T\right)^T [\mu]\left(\nabla\{N\}^T\right) dV \tag{8}$$

$$\left[K^N\right] = \int_V \frac{\partial\mu_h}{\partial|H|}\left(\{H\}^T \nabla\{N\}^T\right)^T \left(\{H\}^T \nabla\{N\}^T\right)\frac{dV}{|H|} \tag{9}$$

where {N} is the element shape functions ($\varphi=\{N\}^T\{\varphi_e\}$) and $\frac{\partial\mu_h}{\partial|H|}$ is the derivative of

permeability with respect to magnitude of the magnetic field intensity.

Figure 3 shows a surface plot of the amplitude of the radial and axial component of magnetic flux density in the vicinity of a rectangular defect whose sizes are length=10mm, width=10mm, and depth=10mm. The two peaks in the amplitude are due to the flux being diverted into and returning from the air around the flaw.

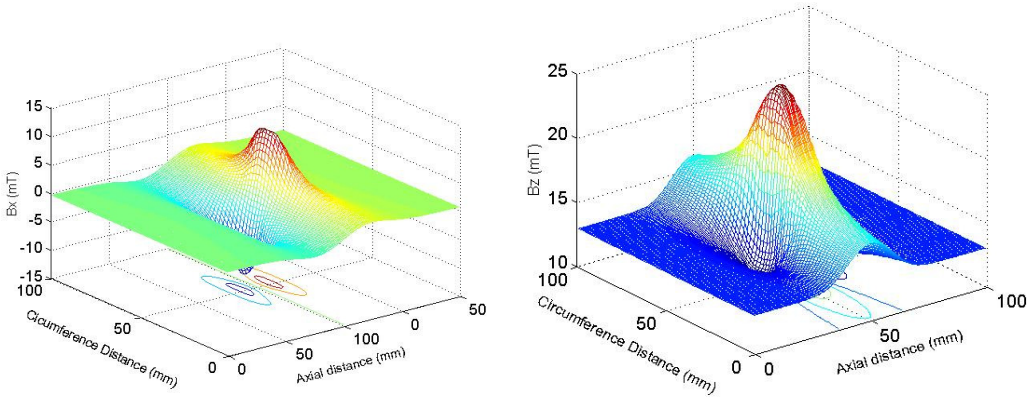

(a) Radial component (b) Axial component

Figure 3. Surface plot of axial magnetic flux density

4. Experiments and Results

The photograph of the MFL measurement system is shown in Figure 4. The apparatus contain a permanent magnet assembly, a DC motor control system, a data acquisition system and other associated units. The permanent magnet assembly includes a magnetic circuit, a hall probe, and a signal pre-procession circuit. There are 16 Hall sensors to measure the leakage flux.

In order to perform this experiment, different artificial defects are made on the specimen whose thickness is 12mm. The defects have diameter of 12mm and their depths are 100%(12mm) , 50%(6mm) 20%(2.5mm), and 10%(1.2mm) , respectively. Figure 5(a) shows the plots of radial component of magnetic flux density and Figure 5(b) shows the plots of axial component of magnetic flux density.

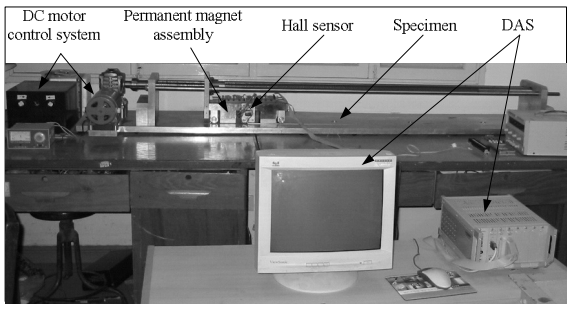

Figure 4. Photograph of the MFL measurements system

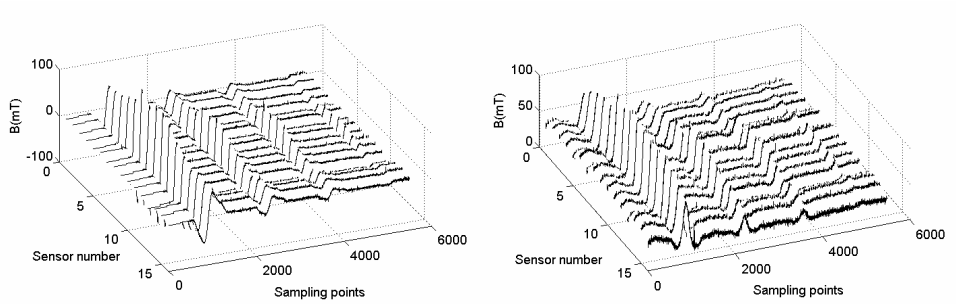

(a) Radial component (b) Axial component

Figure 5. Plot of radial and axial component of magnetic flux density

5. Conclusion

Analytical model can express MFL signal by an equation but it is difficult to deal with realistic defect shapes and the influence of test parameters. Compared with analytical method, numerical model can process different defects shapes, materials, magnetizing situation but it has a more complicated procedure and higher computational cost. Experiment results can validate the simulation of analytical and numerical models, while it difficult to do many experiment due to the high costs and time consuming.

Reference

[1] C Edwards et al,. The magnetic leakage field of surface-breaking cracks, Applied Physics, Volume 19 1986, P657-673

[2] Ichizo Uetake et al,. Magnetic flux leakage by adjacent paraller surface slots, NDT&E International, Volume 30 Number 6, 1997, P371-376

[3] K Mandal et al,. A study of magnetic flux-leakage signals, Applied Physics, Volume 31, 1998, P3211-3217

[4] Mitsuaki Katoh et al,. Modeling of the yoke-magnetization in MFL-testing by finite elements, NDT&E International, Volume 36, 2003, P479–486

[5] P.A.Ivanov et al,. Magnetic Flux Leakage Modeling for Mechanical Damage in Transmission Pipelines, IEEE TRANSACTIONS ON MAGNETICS, Volume 34 Number 5, 1998, P3020-3023

[6] Catalin Mandache et al,. A model for magnetic flux leakage signal predictions, Applied Physics, Volume 36 2003, P2427-2431

[7] Huang Zuoying et al,. 3D FEM analysis in magnetic flux leakage method, NDT&E International, Volume 39 Number 1, 2006, P61-66.